PERGAMON

Journal of Geodynamics 34 (2002) 653–666

JOURNAL OF
GEODYNAMICS

www.elsevier.com/locate/jog

Lateral variations of the modal (a/b) values for the different regions of the world

Yusuf Bayrak, Ahmet Yılmaztürk*, Serkan Öztürk

Department of Geophysics, Karadeniz Technical University, 61080, Trabzon, Turkey

Received 12 November 2001; received in revised form 30 April 2002; accepted 27 May 2002

Abstract

Several catalogues of global earthquakes reported for the time period from 1900 to 2000 have been compiled to examine lateral variations of the modal (a/b) values as derived from the Gutenberg–Richter empirical law. For this purpose, the world was divided into 27 different seismic regions in terms of tectonic environments. The parameters *a* and *b* were calculated using the least-squares method. The modal values computed for each region were used to produce a global map of the modal values using a grid space of 3°. The results show that *a* and *b*-values do not always supply much information about tectonic environments of the different regions. It is observed that the modal values estimated for different tectonic regions are consistent with seismicity of the world and represent global seismic sources better than *a* or *b* values. The highest modal values have been found in the oceanic subduction zones, and the lowest values in the oceanic ridges. Lowest *b* values are observed in trenches. These observations suggest that there is a correlation between apparent stresses and *b* values. Mapping of the modal values provides detailed images of the zones presenting low and high seismic activity and it may be used as a measure of seismic potential sources and relative hazard levels.

1. Introduction

Studying the seismic activity of the world has been done extensively, several researchers calculated different parameters of seismicity by using various methods. The empirical relationship between magnitude and frequency of earthquake occurrences is well known as the Gutenberg–Richter (G–R)

* Corresponding author. Fax: +90-462-325-7405.
E-mail address: yturk@risc01.ktu.edu.tr (A. Yılmaztürk).

0264-3707/02/$ - see front matter
PII: S0264-3707(02)00037-6

relationships. Since Gutenberg and Richter (1944) estimated the parameters a and b, the evaluation of the parameters have been frequently used in statistical calculation of seismicity. The parameter a depends on the seismicity rate which varies greatly from region to region (Olsson, 1999). The parameter b is related to properties of focal material and represents tectonic characteristics of a region (Allen et al., 1965; Hatzidimitriou et al.; 1985, Wang, 1988). Details in the sense of these parameters may be found in Yılmaztürk et al. (1999). Gutenberg and Richter (1954) suggested that the b parameter changes between 0.45 and 1.5, while Miyamura (1962) found that b-values, ranging from 0.4 to 1.8 for different tectonic areas, are larger in the oceanic crust than in the Circum-Pacific and the Alpine orogenic zones. Tsapanos (1990) observed that b-values are between 0.75 and 0.85 for 11 different seismic regions of the world. Several empirical scaling functions based on the parameters of a and b have been proposed for different regions and different time intervals (Kaila et al., 1974; Kaila and Rao, 1975; Bath, 1981; Bender, 1983; Smith, 1986; Christova, 1992; Tsapanos and Papazachos, 1998; Al-Amri et al., 1998; Yılmaztürk et al., 1999).

Recently, Yılmaztürk et al. (1999) and Bayrak et al. (2000) showed that distribution of the modal (a/b) values provide detailed images of the local areas presented by high and low seismic zones in and around Turkey. The main purpose of this study is to calculate the ratio of the parameters a and b from the G–R relations for the different regions of the world and to find relation between the tectonic structures and these values. For this purpose, the world has been divided into different 27 seismic regions and evaluated the parameters of a and b in the G–R relations for each region.

2. Data

The data used in this study have been compiled from several sources. The earthquakes for the time period from 1900 to 1992 come from the Global Hypocenter Data Base CD-ROM prepared by USGS (Unites States Geological Survey). Nine available catalogues (ABE, BCIS, BDA, GREAT, GUTE, ISS, ISSN, P&S, and PDE) including global earthquakes have been compiled using a rectangular search method. The PDE (preliminary determination of epicenters) data and IRIS (Incorporated Research Institutions for Seismology) data, for the time period from 1993 to 2000 are also used to update the database.

An earthquake data set used in seismicity or seismic risk studies must be homogenous and complete. All earthquake magnitudes should be in the same magnitude scale and a specific time period. In order to construct a uniform catalogue, we have used the relations found by Bayrak (1998) for different regions of the world. These empirical relations are based on different magnitude scales (m_b—body wave magnitude, M_S—surface wave magnitude, M_L—local magnitude, M_D—duration magnitude, M_W—moment magnitude, M_N—Nuttli magnitude, M_{UK}—unknown type of magnitude) and intensity. Using those relations we have constructed a uniform catalogue of M_S. The final catalogue consists of about 201,000 earthquakes. Magnitude range varies from 1.0 to 8.6. In Fig. 1, epicenter distributions of the earthquake magnitudes higher than 6.0 are shown by different symbols. Largest earthquakes ($M_S \geqslant 8.0$) occur in the subduction zones and the continental thrust zones. Generally, magnitudes of the earthquakes located in the oceanic regions including transform faults and ridges are lower than 7.0. Several earthquakes for which magnitudes are between 7.0 and 8.0 have occurred in the San Andreas and the North Anatolian Faults.

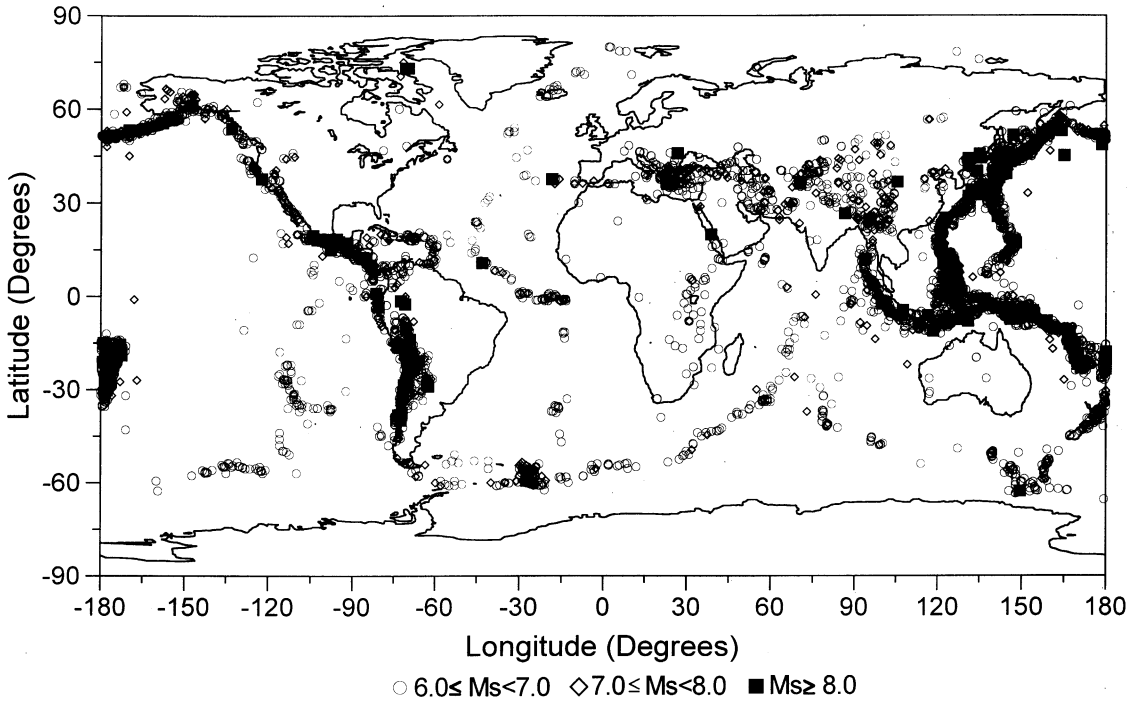

Fig. 1. Epicenter locations of the earthquakes of $M_S \geqslant 6.0$ for the time period 1900–2000. Data for only moderate to large magnitude size of the earthquakes are shown by different symbols.

The world has been divided into 27 different seismic regions in terms of tectonic environments and geographical distribution of the earthquake epicenters. Boundaries of these regions and associated earthquake occurrences with magnitude of 6.0 or above are shown in Fig. 2. Total number of the earthquakes in the regions is about 195,000. The rest of the data is too sparse to characterize the seismic regions. Cut-off magnitudes ($M_{\min}$), percentage of the earthquakes below the $M_{\min}$, the numbers of the earthquakes above the $M_{\min}$ and the locations of the regions are listed in Table 1. Regions of 1, 3, 5, 6, 8, 12, 17, 21–27 are related to the oceanic subduction zones. Regions of 4, 7, 9–11, 13–15 are associated with the oceanic transform faults and ridges. The San Andreas Fault is located in Region 2 and the North Anatolian Fault in region 18. Regions 19 and 20 are associated with continental collision zones. Region 16 represents the Africa rift system.

3. Gutenberg–Richter relationship

The number of earthquakes in any given area during a specific period of observation is a basic representation of seismicity. The frequency of occurrence of earthquakes can be expressed as a function of magnitude.

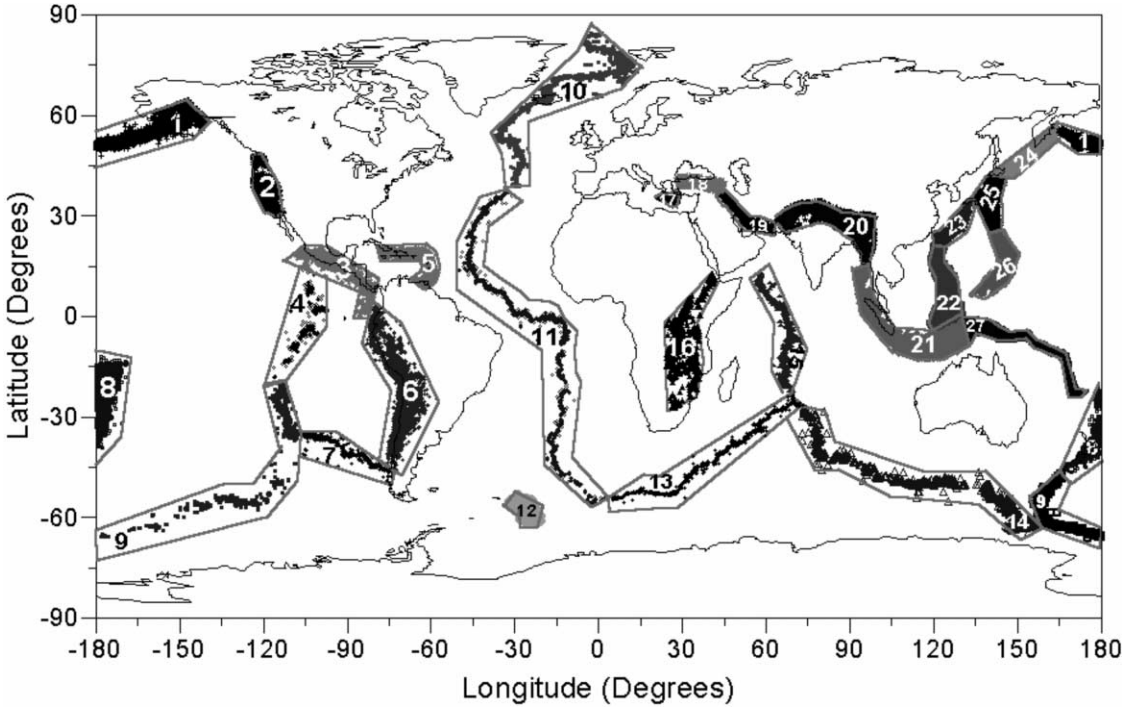

Fig. 2. Boundaries of the seismic regions and epicenter locations of the earthquakes.

$$\mathrm{Log}N = a - bM \tag{1}$$

Where N is cumulative number of earthquakes within a magnitude interval $M \pm \Delta M$, a and b are constants. The constants known as seismicity parameters were first estimated by Gutenberg and Richter (1944) for different regions. The parameter a showing the activity level of seismicity exhibits significant variations from region to region as it depends on the period of observations and area of investigation. The parameter b is related to tectonic characteristic of a region under investigation. For low magnitude seismicity, there is a correlation between the space variations in b values and static stress drop, apparent stress and dynamic stress (Urbancic et al., 1992). However, it should be born in mind that its relative value highly depends, also, on the size of the largest earthquake in a cell.

We have selected different regions of the world to calculate the G–R relationships. These regions are shown in Fig. 2 and listed in Table 1. The least-squares method was used to estimate the a and b-values. Generally, the G–R relationships give a straight line, but the data deviate from a straight line for smaller and larger events. Therefore, the calculations for different regions are restricted to the magnitude range $M_{\min} \leqslant M \leqslant M_{\max}$. The frequency distributions of earthquake magnitudes for each region are displayed in Fig. 3. Percentage of small magnitudes lower than cut-off ($M_{\min}$) values and the estimated a and b-values for the rest of data are given in Table 1. In the graphs, straight lines represent the least-squares fit to all earthquakes and circles represent cumulative number of earthquakes in cells.

Table 1
Information on the data sets used to estimate the Gutenberg-Richter parameters (a and b) for different tectonic regions

Region	M_{min}	% Data below M_{min}	Number of earthquakes above M_{min}	Region	a	b	a/b	TE
1	3.0	83	18,045	Aleutian Trench	6.35	0.63	10.08	OSZ
2	3.0	50	17,421	San Andreas Fault	6.11	0.72	8.49	CT
3	3.5	76	11,338	Mexico Trench	6.08	0.58	10.48	OSZ
4	5.0	20	778	East Pacific Ridge	8.37	1.19	7.03	MOR
5	3.0	74	6386	Caribbean Trench	5.65	0.64	8.83	OSZ
6	3.3	79	17,747	Peru–Chile Trench	5.95	0.53	11.23	OSZ
7	4.8	44	741	Chile Ridge	7.51	1.01	7.44	MOR
8	4.0	79	17,224	Tonga Trench	7.23	0.72	10.04	OSZ
9	4.8	46	1457	Pacific-Antarctic Ridge	7.60	0.95	8.00	MOR
10	4.0	60	3106	Reykjanes Ridge	7.42	0.99	7.49	MOR
11	4.5	53	3510	Mid Atlantic Ridge	7.95	1.00	7.95	MOR
12	4.3	75	1862	Sandwich Trench	6.53	0.74	8.82	OSZ
13	4.3	72	1171	South-West Indian Ridge	6.83	0.86	7.94	MOR
14	4.8	47	1371	South-east Indian Ridge	7.41	0.93	7.97	MOR
15	4.0	85	1314	Mid Indian Ridge	7.14	0.94	7.60	MOR
16	3.8	52	1419	African Rift	5.89	0.73	8.07	Rf
17	3.0	89	3600	Aegean Trench	5.68	0.69	8.23	OSZ
18	2.8	76	1706	North Anatolian Fault	4.80	0.55	8.73	CT
19	3.5	80	2507	Bitlis–Zagros Collision zone	6.37	0.78	8.17	CZ
20	4.0	57	3392	Himalayas Collision Zone	6.17	0.69	8.94	CZ
21	3.8	76	13,755	Sumatra–Java Trench	6.76	0.67	10.09	OSZ
22	3.8	87	14,893	Philippine Trench	6.84	0.68	10.06	OSZ
23	4.0	63	5962	Nonsai Shoto Trench	6.07	0.61	9.95	OSZ
24	4.0	67	13,115	Kurile Trench	6.48	0.63	10.29	OSZ
25	3.5	77	1534	Japan Trench	6.25	0.61	10.25	OSZ
26	3.5	92	4803	Mariana Trench	6.27	0.68	9.22	OSZ
27	4.0	71	24,861	Solomon–New Hebrides Trench	6.63	0.60	11.05	OSZ

MOR: mid-oceanic ridges and transform faults, TE: tectonic environments, OSZ: oceanic subduction zone, CT: continental transform, Rf: rift, CZ: collision zone.

Gutenberg and Richter (1954) suggested that b values range from 0.45 to 1.50 for various region of the world. Tsapanos (1990) calculated b values for 11 seismic regions of the world and observed that b values were between 0.75 and 0.85. This present study reveals that b values change from 0.53 to 1.19 for different regions of the world. Miyamura (1962) observed the largest b values in the oceanic crust. We similarly found high b-values in the mid-oceanic ridges. The values given in Table 1 change from 0.86 to 1.19 in the mid-oceanic ridges and from 0.53 to 0.74 in the oceanic subduction zones. It is also observed that b value is 0.72 in the San Andreas Fault, 0.73 in the Africa Rift system, 0.55 in the North Anatolian Fault, 0.78 in the Bitlis-Zagros collision zone and 0.69 in the Himalayas collision zone. Average b value is 0.64 for the oceanic subduction zones and 0.98 for the mid-oceanic ridges. Choy and Boatwright (1995) show that the lowest apparent stresses are associated with the thrust faulting at subduction zones and the highest apparent stresses with the strike-slip faulting at oceanic ridge transforms. Their results

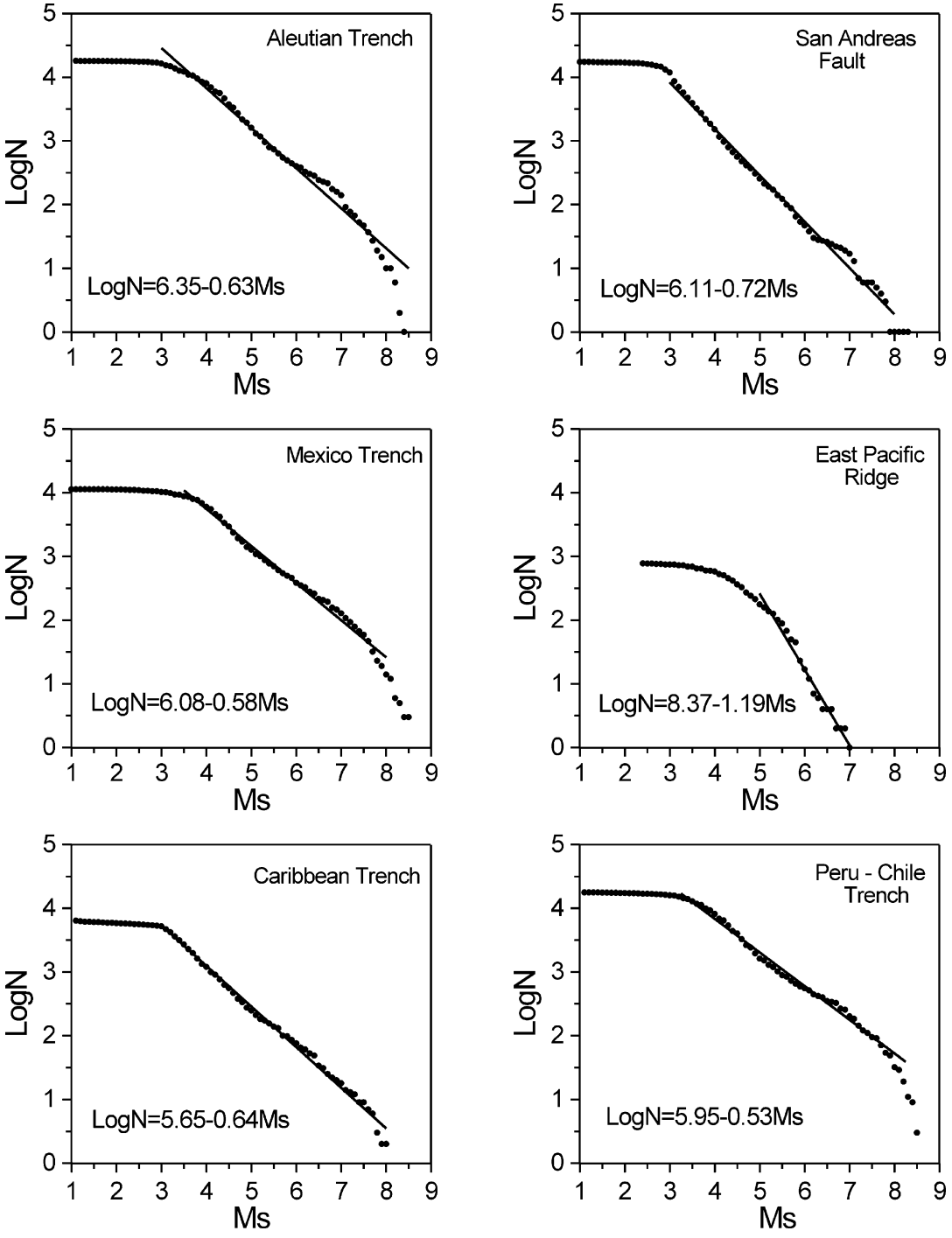

Fig. 3. Cumulative frequency-magnitude distributions of earthquake occurrences for the different 27 regions. Notice that cut-off magnitudes vary from region to region. Linear fits to data points on the curves have been used to estimate the Gutenberg–Richter parameters.

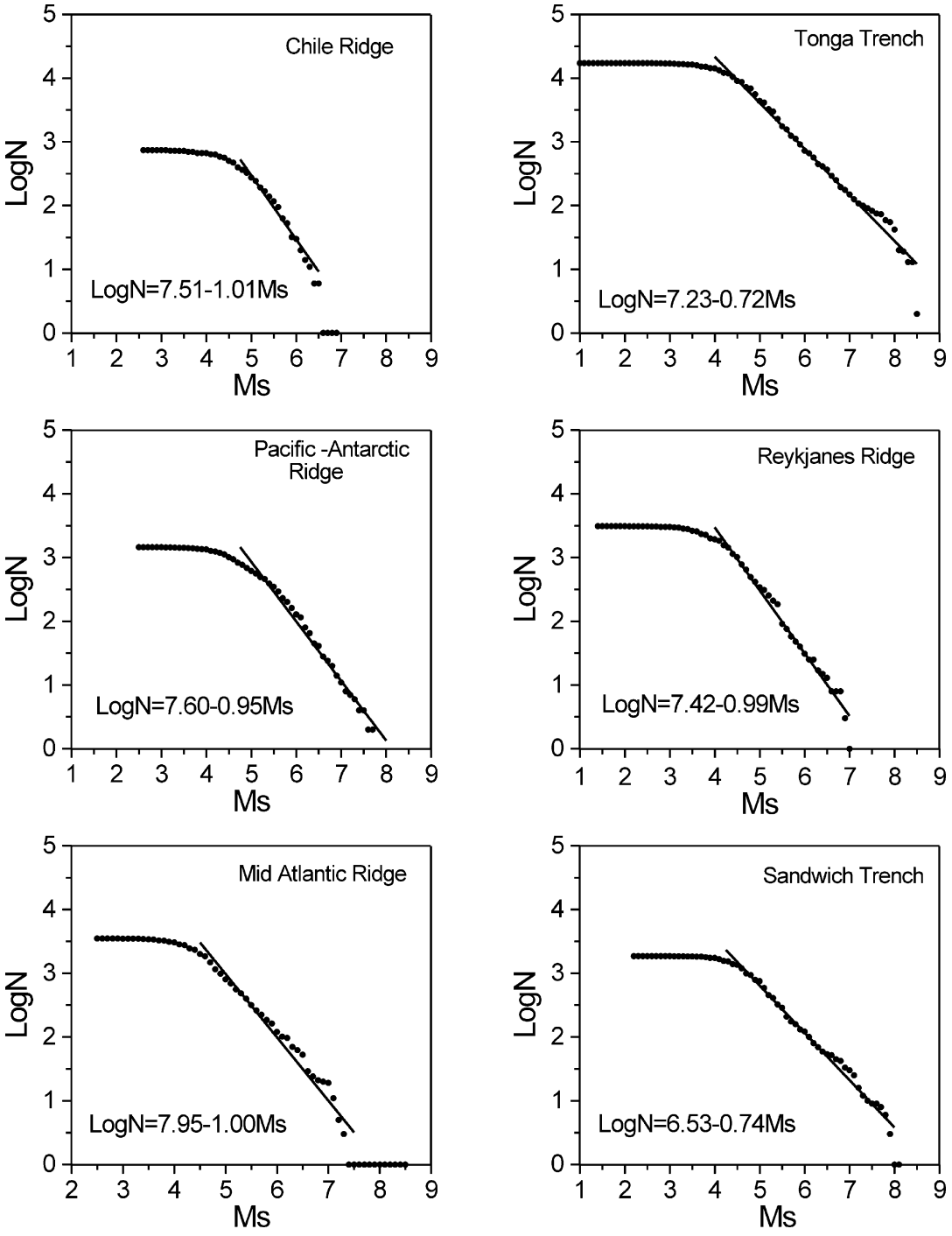

Fig. 3. (*continued*)

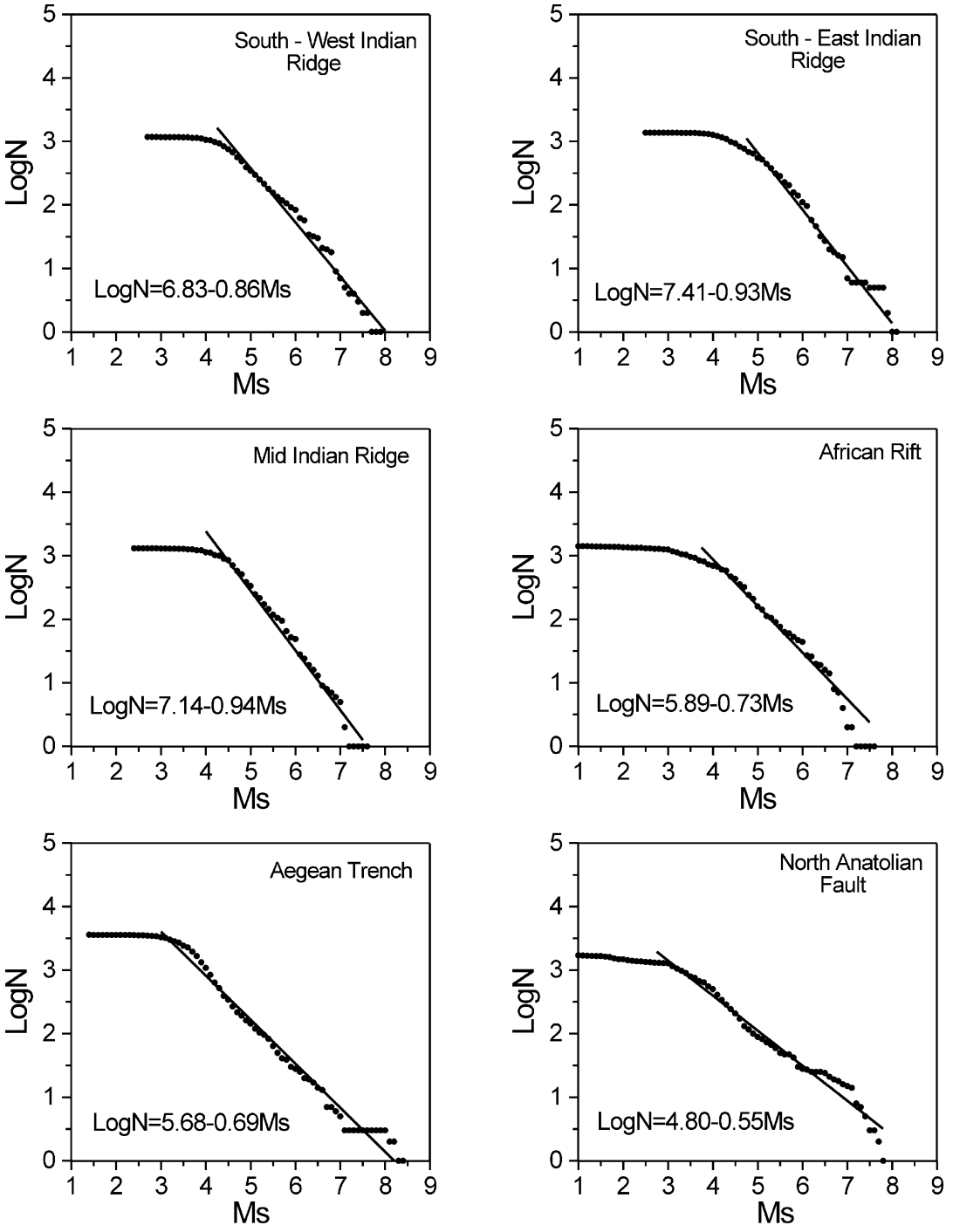

Fig. 3. (*continued*)

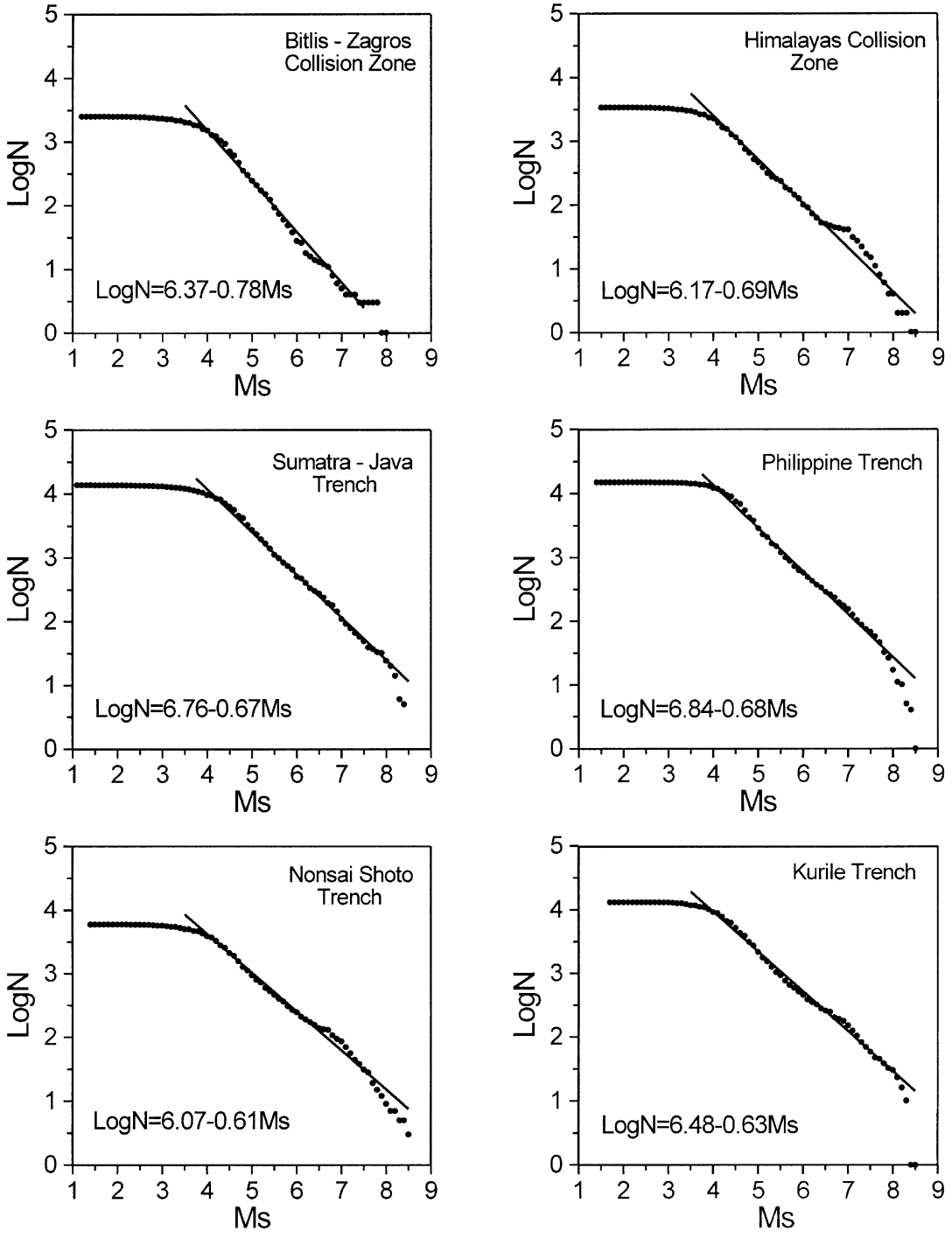

Fig. 3. (*continued*)

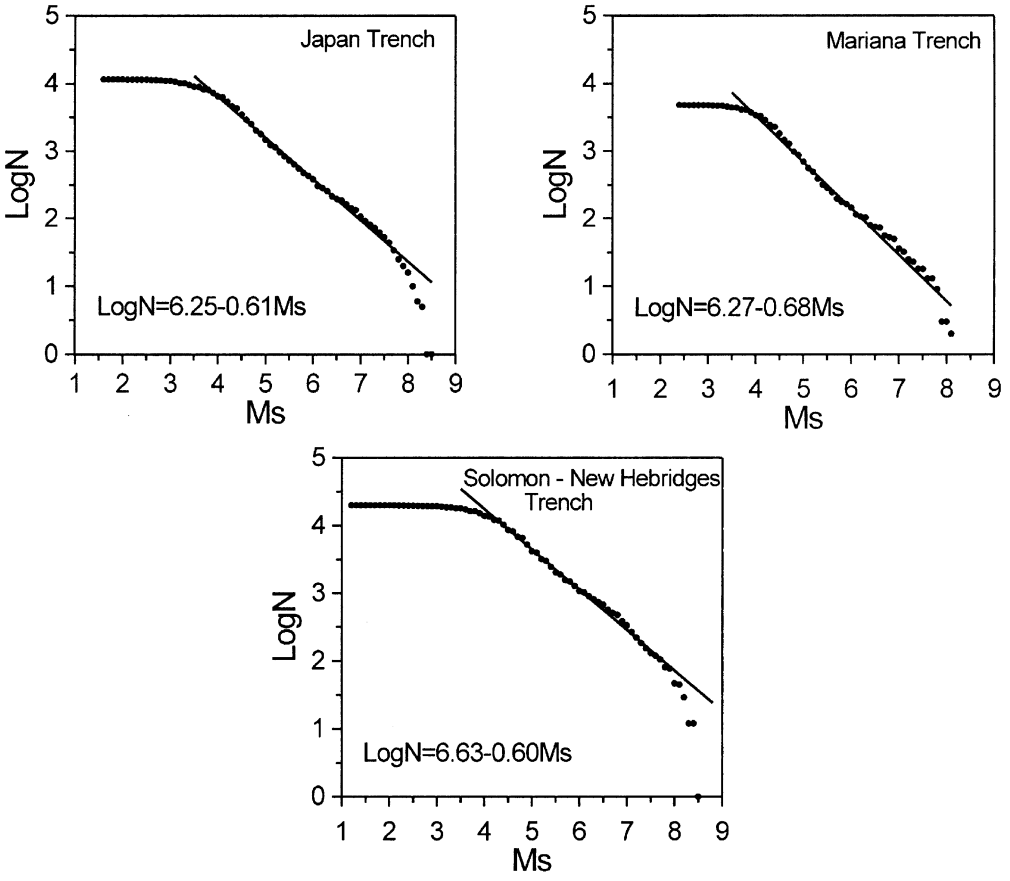

Fig. 3. (*continued*)

seem to agree with b values as obtained, for the same regions, in this study. This is because most of large earthquakes have been occurred in the oceanic subduction zones, thrust zones and continental transforms. Higher b values are observed in the case of no occurrence of large earthquakes. High cut-off magnitudes ($M_{\min}$), also, result in higher b values. It is vice-versa for the presence of large earthquakes or for low cut-off magnitudes. Therefore, b values calculated for the mid-oceanic ridges are higher than those of the oceanic subduction zones.

It is observed that a-values are between 5.65 and 7.23 in the oceanic subduction zones and 6.83 and 8.37 in the mid-oceanic ridges. It is 6.11 in the San Andreas Fault, 5.89 in the Africa Rift system, 4.80 in the North Anatolian Fault, 6.37 in the Bitlis–Zagros collision zone and 6.37 in Himalayas collision zone. Since a-value is related to activity level of seismicity, it is expected that high a values should be observed in the oceanic subduction zones. But, data from the mid-oceanic ridges present high cut-off magnitudes ($M_{\min}$) and result in higher a values. We could not find a systematic relation between different tectonic structures and a values. This is because of large number of small magnitude events deviating from straight lines. Magnitudes for these data range from 3.0 to 4.0 in the oceanic subduction zones and from 4.5 to 5.0 in the mid-oceanic ridges. Cut-off magnitudes ($M_{\min}$) are chosen around these values. Moreover, high cut-off magnitudes

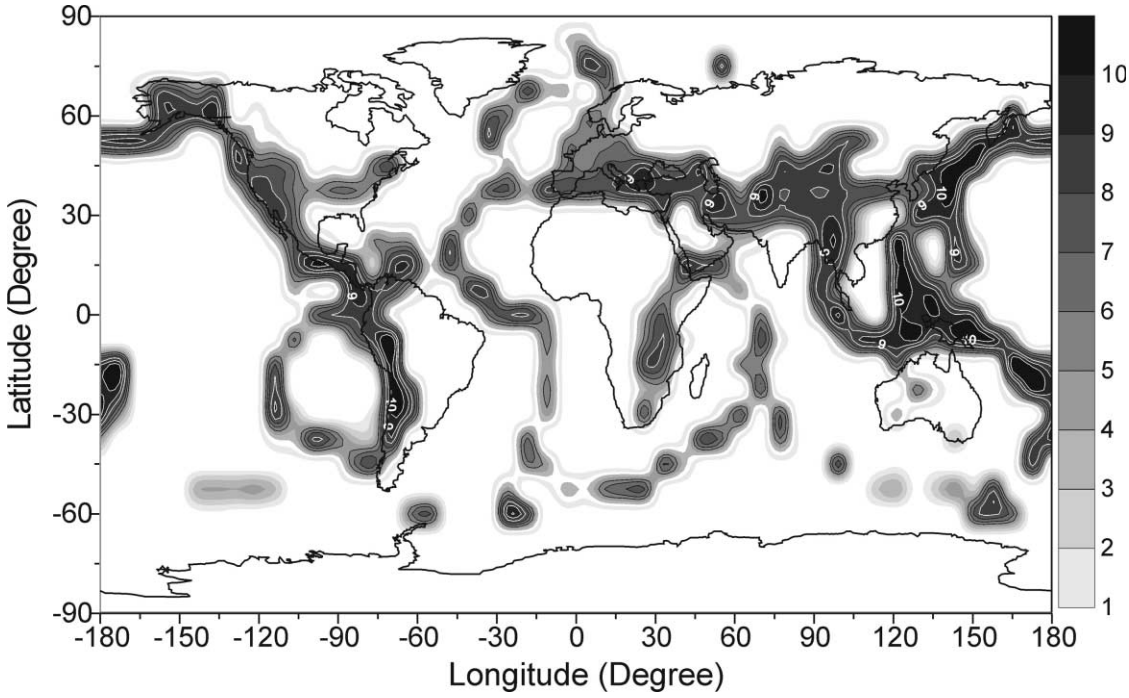

Fig. 4. A contour map of the global modal (a/b) values estimated for a grid of equally spaced points of 3°.

used in the analysis will result in higher *b*-values. As a result, we can suggest that *a* and *b*-values do not always supply much information about different tectonic environments.

4. Modal values for different regions

Yılmaztürk et al. (1999) pointed out to significance of the distribution of the modal (a/b) values, for earthquake occurrences in and around Turkey. In this study, a similar approach has been applied to different regions of the world as shown in Fig. 2. The observed values for each region are given in Table 1. It is found that the modal values change from 8.83 to 11.23 in the oceanic subduction zones and from 7.03 to 8.00 in the mid-oceanic ridges. It is also observed that the a/b ratio is 8.49 for the San Andreas Fault, 8.07 for the Africa Rift system, 8.73 for the North Anatolian Fault, 8.17 for the Bitlis–Zagros collision zone and 8.94 for the Himalayas. An average values of the a/b ratio is about 9.90 in the oceanic subduction zones and 7.68 in the mid-oceanic ridges.

Most of earthquake occurrences in the world are concentrated on the oceanic subduction zones. Largest earthquakes, generally, occur in these zones. For example, four largest recorded earthquakes (1960 Chile, $M_W = 9.5$; 1964 Alaska, $M_W = 9.2$; 1965 Rat Islands, $M_W = 8.7$; and 1963 Kurile Islands, $M_W = 8.5$) have been occurred in those regions (Ruff and Kanamori, 1983). Since the slope of the cumulative regression curve is sensitive to the size of largest earthquake, the highest modal values is observed at these zones. Ruff and Kanamori (1980) found that the largest earthquakes in the world occurred in Chile. A meaningful result is the largest modal value (11.23)

observed for the region 6 including the Peru–Chile Trench. For the mid-oceanic ridges, the largest expected earthquake size is between 7.0 and 7.5 (Lay and Wallace, 1995). The lowest modal values are associated with those ridges. Both the seismicity and the modal values of continental transforms are higher than that of the mid-oceanic ridges. As a result, the modal values estimated for different tectonic environments are consistent with seismicity of the world and reflect global seismic potential sources better than a and b values.

5. Map of the global modal values

Fig. 4 shows geographical distribution of the modal values of earthquakes. In order to produce a global map of the modal values, the whole world is divided into a grid point mesh $3^{o} \times 3^{o}$. The values of a and b were estimated by the least squares method. Then, the a/b values were calculated for each grid and plotted at the center of grids.

It is observed that the largest modal values are related to the oceanic subduction zones where contour level is between 9.0 and 11.0. Bayrak and Yılmaztürk (1999) have shown that higher moment values are associated with thrust faults. Choy and Boatwright (1995) pointed out that lowest apparent stresses have been observed thrust faulting at these zones. This is because of the lower energies or higher moment values resulting in a decrease in the apparent stress. Maximum values are found in the Peru–Chile and the Solomon–New Hebrides Trenches. In the Himalayas and Bitlis–Zagros collision zones, the contour levels are between 8.0 and 10.0. Contours higher than 9.0 are not observed in the North Anatolian Fault and the San Andreas Fault. Generally, the contour levels in the oceanic regions including transform faults and ridges are lower than 8.0.

Since the drawn contour map is consistent with global seismic activity as shown in Fig. 1, there is a systematic variation between tectonic environments and the modal values observed. It is found that the higher modal values are associated with the highest seismic activity observed in the oceanic subduction zones and the lower values are associated with the lowest seismic activity observed in the mid-oceanic ridges. In this sense, a classification of seismic activity of the world in terms of the modal values shows that the oceanic subduction zones are in the first degree of activity, the continental transforms and the thrust zones in the second degree of activity, and the mid-oceanic ridges in the third degree of activity. As a result, the map of the modal values provides detailed images of the different zones presenting low and high seismic activity and it can be used as a seismic hazard map.

6. Conclusions

A homogeneous catalogue has been constructed from the global earthquake data compiled from various sources. Relying on the distribution pattern of the modal (a/b) values helps us to better understand the regional seismic activity in relation to the parameters a and b as derived from the Gutenberg–Richter empirical law. Characteristics of these parameters were discussed in Yılmaztürk et al. (1999).

It seems that there is a correlation between b values and apparent stresses associated with earthquakes in trenches where the modal values are significantly high. Higher seismic moments or

lower seismic energies result in lower apparent stresses. Regions with low apparent stresses are subject to experience with large magnitude earthquakes resulting in low b and high modal values. The highest b values are observed in the mid-oceanic ridges and the lowest values in the oceanic subduction zones. This is because of high cut-off magnitudes, used in the oceanic regions. Since cut-off magnitudes were low in the subduction zones, the a and b values have been calculated lower than expected values. Therefore, there are no systematic variations between a and b values and the tectonic environments as seen in Table 1. It is observed that the modal values calculated for 27 different regions are consistent with tectonic environments and reflect the global seismicity better than a and b values. The highest modal values have been observed in the oceanic subduction zones, while the low values have been observed in the oceanic regions associated with transform faults and ridges. Consequently, the global map of the modal values consistents with the global seismic activity map and may be used to represent seismic potential sources.

References

Al-Amri, A.M.S., Punsalan, B.T., Uy, E.A., 1998. Spatial distribution of the seicmicity parameters in the Red Sea region. Journal of Asian Earth Sciences 16, 557–563.

Allen, C.R., Amand, P.S., Richter, C.F., Nordquist, J.M., 1965. Relation between seismicity and geological structure in the southern California region. Bull. Seism. Soc. Am. 55, 752–797.

Bath, M., 1981. Earthquake recurrence of a particular type. PAGEOPH 119, 1063–1076.

Bayrak, Y., 1998. Global Depremlerin Genel Özellikleri: Farklı Sismik Zonlardaki Deprem Kaynak Parametrelerinin İrdelenmesi (Some aspects of global earthquakes: investigation of earthquakes source parameters in different seismic zones, in Turkish with an English abstracts). PhD thesis, Karadeniz Teknik Üniversitesi, Trabzon, Turkey.

Bayrak, Y., Yılmaztürk, A., 1999. Türkiye ve civarındaki sismik moment ve gerilim dağılımı (seismic moment and stress distribution in and around Turkey, in Turkish with English abstract). Yerbilimleri 21, 1–15.

Bayrak, Y., Erduran, A., Yılmaztürk, A., 2000. Türkiye'deki farklı sismotektonik bölgelerin sismisitesi (Seismicity of the different seismotectonic regions in Turkey). In Turkish with an English abstracts). Ulusal Jeofizik 2000 Toplantısı, pp. 135—138, 23—25, Kasım, Ankara.

Bender, B., 1983. Maximum likelihood estimation of b values for magnitude grouped data. Bull. Seism. Soc. Am. 73 (3), 831–851.

Choy, G.L., Boatwright, J.L., 1995. Global patterns of radiated seismic energy and apparent stress. Geophys. J. Res., 100 (B9) 18, 18,205–18,228.

Christova, C., 1992. Seismicity depth pattern, seismic energy and b value depth variation in the Hellenic Wadati Benioff zone. Phys. Earth Planet. Inter. 72, 38–48.

Gutenberg, B., Richter, C.F., 1944. Frequency of earthquakes in California. Bull. Seism. Soc. Am. 34, 185–188.

Gutenberg, B., Richter, C.F., 1954. Seismicity of the Earth and Associated Phenomena. Princeton Univ. Press, Princeton, NY. pp. 310.

Hatzidimitriou, P.M., Papadimitrou, E.E., Mountrakis, D.M., Papazachos, B.C., 1985. The seismic parameter b of the frequency-magnitude relation and its association with geological zones in the area of Greece. Tectonophysics 120, 141–151.

Kaila, K.L., Rao, N.M., Narain, H., 1974. Seismotectonic maps of southwest Asia region comprising eastern Turkey, Caucasus, Persian Plateau, Afghanistan and Hindu Kush. Bull. Seism. Soc. Am. 64 (3), 657–669.

Kaila, K.L., Rao, N.M., 1975. Seismotectonic maps of European area. Bull. Seism. Soc. Am. 65 (6), 1721–1732.

Lay, T., Wallace, T.C., 1995. Modern Global Seismology. Academic Press, London. pp. 521.

Miyamura, S., 1962. Magnitude-frequency relations and its bearing on geotectonics. Proc. Jap. Acad. 38, 27–30.

Olsson, R., 1999. An estimation of the maximum b-value in the Gutenberg-Richter relation. Geodynamics 27, 547–552.

Ruff, L., Kanamori, H., 1980. Seismicity and subduction process. Phys. Earth Planet. Inter. 23, 240–252.

Ruff, L., Kanamori, H., 1983. Seismic coupling and uncoupling at subduction zones. Tectonophysics 99, 99–117.

Smith, W.D., 1986. Evidence for precursory changes in the frequency-magnitude b-value. Geophys. J. R. Astr. Soc. 86, 815–838.

Tsapanos, T.M., 1990. b-Values of two tectonic parts in circum-Pacific belt. PAGEOPH 134, 229–242.

Tsapanos, T.M., Papazachos, B.C., 1998. Geographical and vertical variation of the earth's seismicity. Journal of Seismology 2, 183–192.

Urbancic, T.I., Trifu C-I, LongJ.M., Young, R.P., 1992. Space-time correlations of b values with stress release. PAGEOPH 139 (3/4), 449–462.

Yılmaztürk, A., Bayrak, Y., Çakır, Ö., 1999. Crustal seismicity in and around Turkey. Natural Hazards 18, 253–267.

Wang, J.-H., 1988. b values of shallow earthquakes in Taiwan. Bull. Seism. Soc. Am. 78 (3), 1243–1254.